

# The Galaxy Luminosity Function during the Reionization Epoch

M. Trenti

*CASA, Department of Astrophysics and Planetary Science, University of Colorado,  
389-UCB, Boulder, CO 80309 USA*

trenti@colorado.edu

and

M. Stiavelli

*Space Telescope Science Institute, 3700 San Martin Drive Baltimore MD 21218 USA*

and

R. J. Bouwens

*Astronomy Department, University of California, Santa Cruz, CA 95064, USA ; Leiden  
Observatory, University of Leiden, Postbus 9513, 2300 RA Leiden, Netherlands*

and

P. Oesch

*Institute of Astronomy, ETH Zurich, CH-8093 Zurich, Switzerland*

and

J. M. Shull

*CASA, Department of Astrophysics and Planetary Science, University of Colorado,  
389-UCB, Boulder, CO 80309 USA*

and

G. D. Illingworth

*Astronomy Department, University of California, Santa Cruz, CA 95064, USA*

and

L. D. Bradley

*Space Telescope Science Institute, 3700 San Martin Drive Baltimore MD 21218 USA*

and

C. M. Carollo

*Institute of Astronomy, ETH Zurich, CH-8093 Zurich, Switzerland*

## ABSTRACT

The new Wide Field Camera 3/IR observations on the Hubble Ultra-Deep Field started investigating the properties of galaxies during the reionization epoch. To interpret these observations, we present a novel approach inspired by the conditional luminosity function method. We calibrate our model to observations at  $z = 6$  and assume a non-evolving galaxy luminosity versus halo mass relation. We first compare model predictions against the luminosity function measured at  $z = 5$  and  $z = 4$ . We then predict the luminosity function at  $z \gtrsim 7$  under the sole assumption of evolution in the underlying dark-matter halo mass function. Our model is consistent with the observed  $z \gtrsim 7$  galaxy number counts in the HUDF survey and suggests a possible steepening of the faint-end slope of the luminosity function:  $\alpha(z \gtrsim 8) \lesssim -1.9$  compared to  $\alpha = -1.74$  at  $z = 6$ . Although we currently see only the brightest galaxies, a hidden population of lower luminosity objects ( $L/L_* \gtrsim 10^{-4}$ ) might provide  $\gtrsim 75\%$  of the total reionizing flux. Assuming escape fraction  $f_{esc} \sim 0.2$ , clumping factor  $C \sim 5$ , top heavy-IMF and low metallicity, galaxies below the detection limit produce complete reionization at  $z \gtrsim 8$ . For solar metallicity and normal stellar IMF, reionization finishes at  $z \gtrsim 6$ , but a smaller  $C/f_{esc}$  is required for an optical depth consistent with the WMAP measurement. Our model highlights that the star formation rate in sub- $L_*$  galaxies has a quasi-linear relation to dark-matter halo mass, suggesting that radiative and mechanical feedback were less effective at  $z \geq 6$  than today.

*Subject headings:* galaxies: high-redshift — early universe — cosmology: theory — stars: formation

## 1. Introduction

The new Wide Field Camera 3/IR (WFC3) Hubble Ultra Deep Field (HUDF09) observations opened a new window on high-redshift galaxy formation (Oesch et al. 2010a,b;

Bouwens et al. 2010a,b; Bunker et al. 2009; McLure et al. 2010; Finkelstein et al. 2009). Yet the sample of  $z \gtrsim 6.5$  galaxies is too small (16 z-dropouts in Oesch et al. 2010b, and 5 Y-dropouts in Bouwens et al. 2010a) for a precise determination of the galaxy luminosity function (LF), especially after taking into account the systematic uncertainty introduced by cosmic variance (Trenti & Stiavelli 2008).

Measuring the galaxy LF is important to assess their contribution to cosmic reionization, which started at  $z \gtrsim 10$ , as inferred from the Thomson scattering optical depth  $\tau_e$  in the CMB background (Komatsu et al. 2009). The nature of the reionizing sources is currently debated. Are normal galaxies the agents of reionization, or are other sources responsible, such as Population III stars or Mini-QSOs (Madau et al. 2004; Sokasian et al. 2004; Shull & Venkatesan 2008)? Within uncertainties, galaxies detected at  $z \sim 6$  barely keep the Universe reionized (Stiavelli et al. 2004b; Bunker et al. 2004). The LF evolution established from  $z \sim 4$  to  $z \sim 6$  (Bouwens et al. 2007) seems to continue into the dark ages, with progressively fewer bright sources (Bolton & Haehnelt 2007; Bouwens et al. 2008, 2010a; Oesch et al. 2009c).

The exploration of the link between LF and underlying dark-matter halo mass function (MF) helps us understand the processes regulating star formation. This has been studied via the conditional luminosity function (CLF) method locally and at high redshift (Vale & Ostriker 2004; Cooray & Milosavljević 2005; Cooray 2005; Cooray & Ouchi 2006; Stark et al. 2007; Bouwens et al. 2008; Lee et al. 2009). Key results are: (1) significant redshift evolution of galaxy luminosity versus halo mass,  $L(M_h)$ , (Cooray 2005; Lee et al. 2009); (2) only a fraction  $\epsilon_{DC} \sim 20 - 30\%$  of halos appears to host Lyman Break galaxies (LBG) (Stark et al. 2007; Lee et al. 2009); (3) the predicted LF at  $z \gtrsim 6$  deviates significantly from Schechter form, missing the sharp drop in density of bright ( $M_{AB} \lesssim -20$ ) galaxies (Bouwens et al. 2008). These findings suggest limitations of the current models extrapolated to the highest redshift. In fact, because of the young age of the Universe during the reionization epoch ( $\Delta z = 1$  corresponds to  $\lesssim 170$  Myr at  $z \gtrsim 6$ ), it becomes difficult to justify rapid evolution of  $L(M_h)$ , unless the IMF changes. A low  $\epsilon_{DC}$  also appears problematic: the halo MF evolves rapidly at  $z \gtrsim 6$ : the number density of  $M_h > 10^{11} M_\odot$  halos (hosting  $\sim L_*$  galaxies) increases by a factor three from  $z = 7$  to  $z = 6$ . Hence,  $\epsilon_{DC} \lesssim 0.3$  implies that the majority of recently formed halos at  $z \geq 6$  did not experience significant star formation. Finally, the absence of a well-defined knee in the predicted  $z \gtrsim 6$  LF differs from the rarity of observed bright galaxies (see Bouwens et al. 2010a).

To overcome these limitations, we present a novel implementation of the CLF model, tailored for application at  $z \gtrsim 5$ . Instead of a duty cycle, we adopt another simple assumption: only halos formed within a given time interval host a detectable LBG (Section 2). Sec-

tion 3 contains the predictions for the  $z \gtrsim 7$  LF, compared to WFC3-HUDF09 observations. Section 4 discusses the contribution of galaxies to reionization.

## 2. An Improved CLF Model for $z \sim 6$

We adopt a variation on the CLF approach (Vale & Ostriker 2004; Cooray & Milosavljević 2005) to construct an empirical relation between the galaxy LF and the halo MF at redshift  $z = 6$ , close to the reionization epoch and with a well measured LF function. In the standard CLF method,  $L(M_h)$  is derived assuming that each dark-matter halo hosts a single galaxy and equating the number of galaxies with luminosity greater than  $L$  to the number of halos with mass greater than  $M_h$  (optionally with  $\epsilon_{DC} \leq 1$ ):

$$\epsilon_{DC} \int_{M_h}^{+\infty} n(M_H, z) dM_H = \int_L^{+\infty} \phi(L, z) dL. \quad (1)$$

Here,  $n(M_h, z)$  is the Sheth & Tormen (1999) halo MF, constructed assuming a WMAP5 cosmology ( $\Omega_\Lambda = 0.72$ ,  $\Omega_m = 0.28$ ,  $\Omega_b = 0.0462$ ,  $\sigma_8 = 0.817$ ,  $n_s = 0.96$ ,  $h = 0.7$ ; Komatsu et al. 2009) and  $\phi(L, z)$  is the galaxy LF at redshift  $z$ .

In our Improved CLF (ICLF) model, rather than  $\epsilon_{DC} < 1$ , we modify Equation 1 to include only halos with  $M \geq M_h$  that have been formed within time interval  $\Delta t$ :

$$\Delta N(M_h, z) = \int_{M_h}^{+\infty} [n(M_H, z) - n(M_H, z_{\Delta t})] dM_H, \quad (2)$$

where  $\Delta t = t_H(z) - t_H(z_{\Delta t})$ , with  $t_H(z)$  being the local Hubble time (Equation 6 of Trenti & Stiavelli 2009). Equation 2 defines an effective duty-cycle  $\epsilon_{DC}^{(eff)}(M_h, z)$ :

$$\epsilon_{DC}^{(eff)}(M_h, z) = \frac{\int_{M_h}^{+\infty} [n(M_H, z) - n(M_H, z_{\Delta t})] dM_H}{\int_{M_h}^{+\infty} n(M_H, z) dM_H}. \quad (3)$$

$L(M_h)$  is defined implicitly by:

$$\epsilon_{DC}^{(eff)}(M_h, z) \int_{M_h}^{+\infty} n(M_H, z) dM_H = \int_L^{+\infty} \phi(L, z) dL. \quad (4)$$

In the limit  $\Delta t \rightarrow +\infty$  and  $\epsilon_{DC} = 1$ , Equation 4 is equivalent to Equation 1. We adopt  $\Delta t = 200$  Myr but discuss model predictions for  $\Delta t = (100 - 300)$  Myr. The timescale  $\Delta t$  refers to the global evolution of the halo MF (Equations 2-3) and captures the fraction of halos that experienced a recent change in their mass. This ensemble includes halos that

have likely experienced a recent star-formation burst, and are thus more likely to host a UV-bright galaxy. However, for an individual halo star formation is extended over timescales longer than  $\Delta t$  at a lower mass scale. In fact, using our Extended-Press-Schechter modeling (Trenti & Stiavelli 2008; Trenti et al. 2008), we infer that a  $M_h = 10^{11} M_\odot$ ,  $z = 6$  halo had  $M_h > 10^8 M_\odot$ , at  $z > 24$  ( $> 99\%$  confidence). This is consistent with the abundant supply of cold gas present at high-redshift (Kereš et al. 2005; Davé et al. 2008), which suggests sustained star formation over several  $10^8$  yr. In fact, our ICLF model has a higher  $\epsilon_{DC}^{(eff)}(M_h, z)$  at  $z \geq 6$  (Figure 1) than the fixed  $\epsilon_{DC}$  assumed/derived in similar studies (Stark et al. 2007; Lee et al. 2009).

We parametrize the observed LF as a Schechter function:

$$\phi(L) = \frac{\phi_*}{L_*} \left( \frac{L}{L_*} \right)^\alpha \exp(-L/L_*). \quad (5)$$

We calibrate the model to the rest-frame UV parameters measured by Bouwens et al. (2007) for i-dropouts ( $z \sim 6$ ):  $\phi_* = 1.4 \times 10^{-3} \text{ Mpc}^{-3}$  ( $h = 0.7$ ),  $\alpha = -1.74$ ,  $L_* = 10^{-M_*/2.5}$  with  $M_* = -20.24$  (see also Table 1). In Equations 1 and 4, we do not consider scatter in  $L(M_h)$  because we are primarily interested in the insensitive faint end of the relation (Cooray & Milosavljević 2005). We also neglect multiple halo occupation, motivated by current  $z = 6$  observational limits. Only halos with  $M_h \gtrsim 7 \times 10^{11} M_\odot$  are likely to host multiple galaxies (Wechsler et al. 2001). Such halos are rare within a single ACS field of view ( $\lesssim 1$  expected in the  $\sim 3 \times 10^4 \text{ Mpc}^3$  ACS volume for i-dropouts). Halos hosting multiple galaxies are present in surveys at  $z \gtrsim 6$  with a larger volume such as the GOODS field, but their depth is insufficient to detect the fainter (sub- $L_*$ ) satellite galaxies. The model of Lee et al. (2009) provides an independent confirmation.

Figure 1 shows the  $L(M_h)$  relation at  $z = 6$  from Equations 1-4. The faintest galaxies ( $M_{AB} \lesssim -18$ ) live in  $M \gtrsim 2 \times 10^{10} M_\odot$  halos. The blue-shaded region represents the uncertainty derived by varying the LF parameters within the  $1\sigma$  confidence regions in Figure 3 of Bouwens et al. (2007). We included an additional 12% uncertainty in  $\phi_*$  from cosmic variance ( $\sim 21\%/\sqrt{3}$  for the three quasi-independent HUDF05-ACS fields, see Trenti & Stiavelli 2008<sup>1</sup>).  $L(M_h)$  is similar for both models. The steep faint-end slope of the observed LF ( $\alpha \sim -1.7$ ) implies a flattening of  $L(M_h)$  compared to the local Universe, where  $L \propto M_h^4$  (Cooray & Milosavljević 2005). For the standard CLF model we derive  $L \sim M_h^{1.6}$ , while the ICLF model gives  $L \sim M_h^{1.3}$ . This means that the specific star formation efficiency  $\eta$  in small-mass halos depends mildly on halo mass ( $\eta \sim M_h^{0.3}$ ), compared to the strong suppression ( $\eta \sim M_h^3$ ) inferred at  $z = 0$ . This provides clues to the processes that regulate early-time

---

<sup>1</sup>Cosmic variance calculator available at <http://casa.colorado.edu/~trenti/CosmicVariance.html>

star formation, suggesting a scenario where radiative and supernova feedback were less efficient than today. The UV background decreases at  $z > 4$  (Haardt & Madau 1996), likely reducing the impact of photoionization. In addition, halos were more compact, making gas expulsion more difficult.

From the  $L(M_h)$  relation, combined with the measure of the total stellar mass in  $z = 6$  galaxies based on SED fits (Stark et al. 2009; Gonzalez et al. 2010; Labbé et al. 2009), we derive a typical star formation efficiency  $\eta(M_h = 10^{11} M_\odot) \sim 0.06$  (6% of gas converted into stars) with a large uncertainty, driven by the measure of the stellar mass (Figure 9 in Stark et al. 2009). Lower-mass halos are slightly less efficient at converting gas into stars. For example, halos with  $M_h \sim 10^8 M_\odot$ , have  $\eta \sim 0.06 \times (10^8/10^{11})^{0.3} \lesssim 10^{-2}$ , consistent with assumptions in numerical models at  $z \gtrsim 6$  (Trenti & Stiavelli 2009; Trenti et al. 2009). The decrease in  $\eta$  with decreasing halo mass is possibly related to suppression of star formation by local photoionization (Cantalupo 2010).

From  $L(M_h)$  we infer a halo mass  $M_h \gtrsim 8 \times 10^{10} M_\odot$  for galaxies with  $M_{AB} \leq -19.5$ . This agrees with clustering measurements at  $z = 5$  and  $z = 6$  (Overzier et al. 2006).

## 2.1. Validation of the ICLF Model

To validate the predictions of our ICLF model under the sole assumption of evolution in the underlying dark-matter MF, we apply  $L(M_h)$  derived at  $z = 6$  to  $\Delta N(M_h, z)$  at  $z = 4$  and  $z = 5$ . The resulting LFs are reported in Table 1 and Figure 2, and compared to those obtained with the standard CLF method. As expected from past studies (Cooray 2005; Lee et al. 2009), the standard CLF model fails to match the observed LF at  $z \leq 5$  primarily because of strong evolution in  $\phi_*$  [ $\phi_*(z = 4)/\phi_*(z = 6) \sim 2.4$ ]. The ICLF model predicts instead quasi-constant  $\phi_*$ , because the comoving formation rate per unit time for halos hosting faint ( $L \lesssim L_*$ ) galaxies remains approximately constant between  $z = 6$  and  $z = 4$ . The ICLF results are fully consistent with the observed  $z = 5$  LF, and with the bright-end at  $z = 4$ . However, the faint-end slope at  $z = 4$  is underestimated at  $\sim 3\sigma$  (predicted  $\alpha \gtrsim -1.6$  versus  $\alpha = -1.73 \pm 0.05$  measured). This clearly indicates that our simple assumption  $\Delta t = 200$  Myr is no longer valid at  $z \lesssim 4.5$  because  $\epsilon_{DC}^{eff}$  becomes too small at the faint end (Figure 1).

### 3. Luminosity Function Evolution and HUDF09 Dropouts

The current sample of  $z \gtrsim 6.5$  galaxy candidates is too small to provide an independent fit of the LF. For example, Oesch et al. (2010b) measured the  $z \sim 7$  faint-end slope assuming a fixed value for  $\phi_*$  and  $M_*$ . Here, we apply our ICLF model for a full prediction of the  $z \geq 7$  LF. We do not allow evolution of  $L(M_h)$ . Significant redshift evolution is present (Figure 2), simply because there is progressively less structure at higher  $z$ . The decrease in  $\phi_*$  is smaller than predicted by the CLF method. Both models predict a dimming in  $M_*$  ( $\partial M_*/\partial z \sim 0.25$ ) and a steepening of the faint-end slope, which becomes close to  $\alpha = -2$  by  $z = 9$ . The LF evolution is directly related to evolution of the halo MF shape, which depends exponentially on  $M_h$ . As redshift increases, massive halos become rarer, and the relative abundance of smaller mass halos increases.

To have an accurate comparison between predicted and observed number counts, we convolve the LF with the effective volume of the observations as measured with artificial source recovery simulations (Oesch et al. 2010b; Bouwens et al. 2010a). This is crucial because of significant incompleteness at  $-19 \lesssim M_{AB} \lesssim -18$ . These numbers are reported in Table 2 and include two additional ICLF models with  $\Delta t = 100$  Myr and  $\Delta t = 300$  Myr. The counts expected from our reference ICLF model agree remarkably well with the number of sources observed in the HUDF:  $13.4 \pm 5.8$  z-dropouts are predicted (with  $1\sigma$  uncertainty including cosmic variance) in agreement with the 16 candidates of Oesch et al. (2010b). The ICLF models with  $\Delta t = 100 - 300$  Myr are also consistent with the data at  $1\sigma$ . No LF evolution from  $z = 6$  predicts 31 sources (rejected at  $\sim 95\%$  confidence level), while the standard CLF model gives 9.8 sources (rejected at  $\sim 90\%$  confidence). For Y-dropouts, our reference ICLF model gives 5.3 sources at  $z \sim 8$  (compared to 24 without LF evolution), again fully consistent within  $1\sigma$  with the 5 Y-dropout candidates of Bouwens et al. (2010a).

### 4. Consequences for Reionization

With our LF model we can investigate the role of galaxies in the reionization of the Universe. Despite large differences in the estimate of reionizing photon production, past studies established that sources below the current detection limit likely provide a significant fraction of the photon budget. The precise number of ionizing photons thus depends on the minimum luminosity chosen for the extrapolation of the LF. Our modeling offers a physically motivated cut-off for the luminosity of the smallest halo capable of forming stars. Theoretical and numerical investigations establish that a halo at  $z \lesssim 10$  irradiated by a UV field comparable to the one required for reionization needs a mass  $M_h \gtrsim (0.6 - 1.7) \times 10^8 M_\odot$  (virial temperature  $T_{vir} \gtrsim (1 - 2) \times 10^4$  K at  $z = 7$ ) in order to cool and form

stars (Tegmark et al. 1997). For  $T_{vir} \gtrsim 2 \times 10^4$  K, the minimum halo mass corresponds to  $M_{AB} \approx -10$  based on the  $L(M_h)$  relation at  $z = 6$ . Galaxies below the HUDF09 magnitude limit  $M_{AB} \sim -18$  contribute  $\gtrsim 75\%$  of the total luminosity density at  $z = 7$  integrated to  $M_{AB} = -10$ , unless feedback stronger than seen in cosmological simulations (e.g., Ricotti et al. 2008) induces a flattening of the LF below the HUDF09 detection limit.

To evaluate the likelihood that galaxies ionize the universe, we resort to the widely used conversion of luminosity density in star formation rate (SFR; Equation 2 in Madau et al. 1998). We compare this SFR (Figure 3) to the critical rate (Madau et al. 1999) required for reionization,

$$(SFR)_{crit} \sim 0.01 \left( \frac{0.5}{f_{esc}} \right) \left( \frac{C}{5} \right) \left( \frac{1+z}{8} \right)^3 M_{\odot} \text{ yr}^{-1} \text{ Mpc}^{-3}, \quad (6)$$

where  $f_{esc}$  is the escape fraction of ionizing photons and  $C$  the hydrogen clumping factor. Both Equation 2 in Madau et al. (1998) and Equation 6 above depend on explicit assumptions on the stellar IMF (Salpeter 1955 in  $[0.1 : 100]M_{\odot}$ ) and metallicity (Solar). Equation 6 has a large uncertainty, including the IMF-dependent efficiency of Lyman-Continuum photon production. We adopt  $f_{esc} \gtrsim 0.2$ , consistent with the very blue UV slope of small  $z = 7$  galaxies (Bouwens et al. 2010b), and  $C \sim 5$  (Bolton & Haehnelt 2007; Pawlik et al. 2009). Figure 3 shows that  $z \lesssim 7$  galaxies with  $M_{AB} \leq -10$  produce enough photons to reionize the Universe.

To obtain the evolution of the reionization fraction,  $\xi(z)$ , we follow a complementary approach (see Equation 9 and its derivation in Stiavelli et al. 2004a). We adopt an IGM temperature  $T = 2 \times 10^4$  K, include the effect of Helium ( $\text{He}/\text{H} = 0.083$ ) and assume conservatively  $f_{esc} = 0.2$ ,  $C = 5$ , and no ionizing flux at  $z \geq 9.5$ . The production rate of ionizing photons is obtained from the LF by assuming different SEDs for the sources. Figure 3 shows that if the LF is integrated to  $M_{AB} = -10$ , reionization by  $z \sim 6$  is achieved for any SED, including the unlikely scenario with Salpeter IMF and  $Z = Z_{\odot}$  (consistent with the  $(SFR)_{crit}$  analysis). However, in this case, the optical depth to reionization is underestimated compared to the WMAP5 measurement because of the sharp drop of  $\xi(z)$  at  $z \gtrsim 7$  ( $\tau_e \sim 0.05$  versus  $(\tau_e)_{WMAP} = 0.084 \pm 0.016$  [Komatsu et al. 2009]). Metal-poor and top-heavy SEDs alleviate this problem, as they achieve complete reionization at  $z \gtrsim 8$ , predicting  $\tau_e \gtrsim 0.07$ . Alternatively,  $C/f_{esc} \lesssim 10$  is needed. Without a steeper faint-end,  $\alpha(z \geq 6) = -1.74$ , the  $z = 8$  ionizing flux is reduced by  $\sim 40\%$ , requiring a corresponding decrease in  $C/f_{esc}$  for a constant  $\tau_e$ . Without the contribution from sources below the HUDF detection limit (i.e., LF integration to  $M_{AB} = -18$ ), only a top-heavy and metal-poor SED can reionize the universe by  $z = 6$ , but that model predicts  $\tau_e \sim 0.05$ .

## 5. Conclusions

In this Letter we construct a model for the evolution of the galaxy luminosity function at  $z \gtrsim 4.5$  based on a modification of the CLF method. We derive the relation between galaxy luminosity and dark-matter halo mass at  $z = 6$ , assuming a one-to-one correspondence between observed galaxies and halos that formed in a period  $\Delta t = 200$  Myr. Using  $L(M_h)$  fixed at  $z = 6$ , we derive the expected LFs between  $z = 4$  and  $z = 9$ , assuming only evolution of the underlying dark-matter MF. The  $z = 5$  LF is consistent with observations, but our model is less accurate at lower redshift because it underestimates the faint-end slope. At  $z \gtrsim 6$ , we predict a moderate decrease of  $\phi_*$ , a possible steepening of the faint-end slope, and continued evolution of  $L_*$  toward lower values (Figure 2 and Table 1). At all epochs, our predicted LF is well fitted by a Schechter function with a prominent “knee”.

The predicted number counts for the HUDF09-WFC3 field are a good match to the dropouts observed at  $z \sim 7$  and  $z \sim 8$  (Table 2). Overall our ICLF model is consistent with the observed galaxy LF from  $z \sim 5$  to  $z \sim 8$  with no evolution in  $L(M_h)$ . DM halos assembly can explain LF evolution at  $z \geq 5$  without invoking a change in the properties of LBG star formation. This is in agreement with the constant specific star formation rate inferred at  $z \gtrsim 5$  (Gonzalez et al. 2010).

Our model provides evidence for a reduced impact of feedback in low-mass  $z \gtrsim 5$  halos. In fact, we derive a star formation efficiency weakly dependent on halo mass ( $\eta \propto M_h^{0.3}$ ), compared to the strong quenching of star formation derived at  $z = 0$  ( $\eta \propto M_h^3$ ; Cooray & Milosavljević 2005), providing a testable prediction for cosmological simulations. The strong suppression of star formation in  $M_h \lesssim 10^{11} M_\odot$  halos suggested by Bouché et al. (2010) and Maiolino et al. (2008) contrasts with  $\alpha(z = 6) \sim 1.7$  measured for halos with  $M_h \gtrsim 2 \times 10^{10} M_\odot$  (Section 2). Such strong feedback would also imply that galaxies appear incapable of sustaining reionization. In fact, with a steep LF, sources below the HUDF-WFC3 detection limit may contribute  $\gtrsim 75\%$  of the ionizing flux, sufficient for full reionization if  $C/f_{esc} \lesssim 25$ . A metal-poor and top-heavy IMF, or smaller  $C/f_{esc}$ , are required to complete reionization at  $z \gtrsim 8$  for consistency with  $(\tau_e)_{WMAP}$ . While our extrapolation is physically motivated to  $T_{vir} \geq 2 \times 10^4$  K, it extends for 8 magnitudes. Deeper observations are thus crucial to verify that the LF faint-end remains steep.

We thank the referee for useful suggestions. This work is supported by grants NASA-ATP-NNX07AG77G, NSF-AST-0707474, STScI-HST-GO-11563, STScI-HST-GO-11700, JWST-IDS-NAG5-12458 and by the Swiss National Science Foundation.

## REFERENCES

- Bouché N. et al. 2010, ApJ, submitted, arXiv:0912.1858
- Bolton, J. S. & Haehnelt, M. G. 2007, MNRAS, 382, 325
- Bouwens, R. J. et al. 2007, ApJ, 670, 928
- . 2008, ApJ, 686, 230
- Bouwens, R. J. et al. 2010a, ApJ, 709, 133
- Bouwens, R. J. et al. 2010b, ApJ, 708, 69
- Bouwens, R. J. et al. 2004, ApJ, 606, L25
- Bunker, A. et al. 2009, arXiv:0909.2255
- Bunker, A. J. et al. 2004, MNRAS, 355, 374
- Cantalupo, S. 2010, MNRAS, in press,
- Cooray, A. 2005, MNRAS, 364, 303
- Cooray, A. & Milosavljević, M. 2005, ApJ, 627, L89
- Cooray, A. & Ouchi, M. 2006, MNRAS, 369, 1869
- Davé, R. et al. 2008, MNRAS, 391, 110
- Finkelstein, S. L. et al. 2009, arXiv:0912.1338
- Gonzalez, V. et al. 2010, ApJ, in press, arXiv:0909.3517
- Haardt, F. & Madau, P. 1996, ApJ, 461, 20
- Hopkins, P. F. & Elvis, M. 2009, MNRAS, 1516
- Kereš, D. et al. 2005, MNRAS, 363, 2
- Komatsu, E. et al. 2009, ApJS, 180, 330
- Labbé, I. et al. 2009, arXiv:0910.0838
- Lee, K. S. et al. 2009, ApJ, 695, 368
- Madau, P. et al. 1999, ApJ, 514, 648

- Madau, P. et al. 1998, *ApJ*, 498, 106
- Madau, P. et al. 2004, *ApJ*, 604, 484
- Maiolino et al. 2008, *A&A*, 488, 463
- McLure, R. J. et al. 2010, *MNRAS*, in press, arXiv:0909.2437
- Oesch, P. A. et al. 2010a, *ApJ*, 709, 21
- Oesch, P. A. et al. 2010b, *ApJ*, 709, 16
- Oesch, P. A. et al. 2009c, *ApJ*, 690, 1350
- Overzier, R. A. et al. 2006, *ApJ*, 648, L5
- Pawlik, A. H. et al. 2009, *MNRAS*, 394, 1812
- Ricotti M. et al. (2008), *ApJ*, 685, 21
- Salpeter, E. E. 1955, *ApJ*, 121, 161
- Schaerer, D. et al. 2003, *A&A*, 397, 527
- Sheth, R. K. & Tormen, G. 1999, *MNRAS*, 308, 119
- Shull, J. M. & Venkatesan, A. 2008, *ApJ*, 685, 1
- Sokasian, A., et al. 2004, *MNRAS*, 350, 47
- Stark, D. P. et al. 2007, *ApJ*, 668, 627
- Stark, D. P. et al. 2009, *ApJ*, 697, 1493
- Stiavelli, M. et al. 2004a, *ApJ*, 600, 508
- . 2004b, *ApJ*, 610, L1
- Tegmark, M. et al. 1997, *ApJ*, 474, 1
- Trenti, M. & Stiavelli, M. 2007, *ApJ*, 667, 38
- . 2008, *ApJ*, 676, 767
- . 2009, *ApJ*, 694, 879
- Trenti, M. et al. 2008, *ApJ*, 687, 1

Trenti, M. et al. 2009, ApJ, 700, 1672

Vale, A. & Ostriker, J. P. 2004, MNRAS, 353, 189

Wechsler, R. H. et al. 2001, ApJ, 554, 85

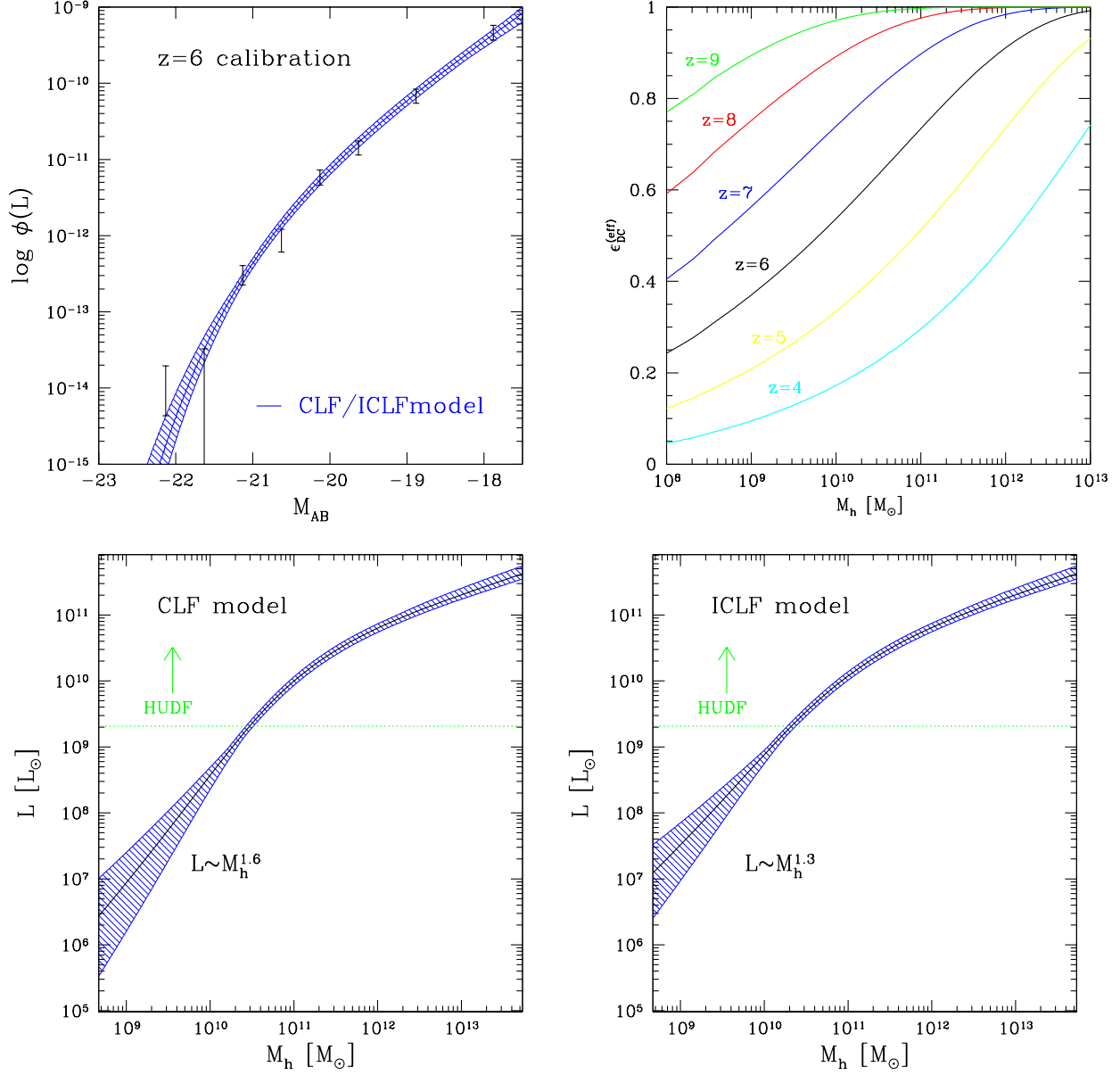


Fig. 1.— Upper Right: Calibration of the CLF/ICLF models with the Bouwens et al. (2007) LF ( $z = 6$ ). Upper Left:  $\epsilon_{DC}^{(eff)}(M_h, z)$  for ICLF model ( $\Delta t = 200$  Myr). Lower panels: Galaxy luminosity versus dark-matter halo mass at  $z = 6$  (black solid line, with blue-shaded area representing the 68% confidence region). Green-dotted line indicates luminosity limit  $z = 6$  observations in the HUDF. Left CLF, right ICLF.

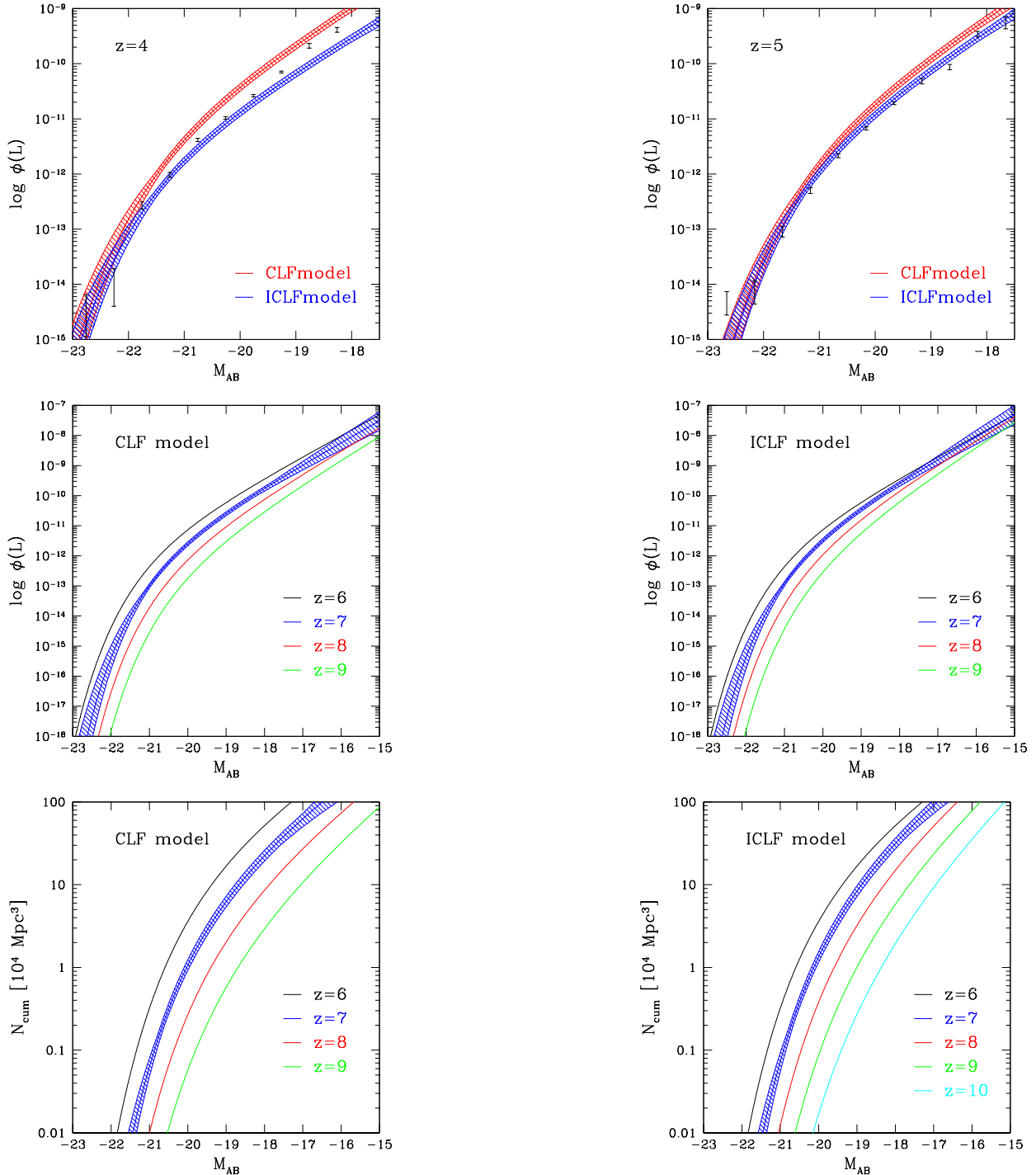


Fig. 2.— Upper panels: Model comparison (red CLF, blue ICLF) at  $z = 4$  (left) and  $z = 5$  (right) with Bouwens et al. (2007) LF (black points). Central panels: LF (black:  $z = 6$ ; blue  $z = 7$ ; red  $z = 8$ ; green  $z = 9$ ) obtained with CLF method (left) and our ICLF model (right). Lower panels: cumulative number of galaxies for a comoving volume of  $10^4 \text{ Mpc}^3$  ( $h = 0.7$ ), similar to HUDF09 field. Blue-shaded area gives  $1\sigma$  confidence region (shown for  $z = 7$  only).

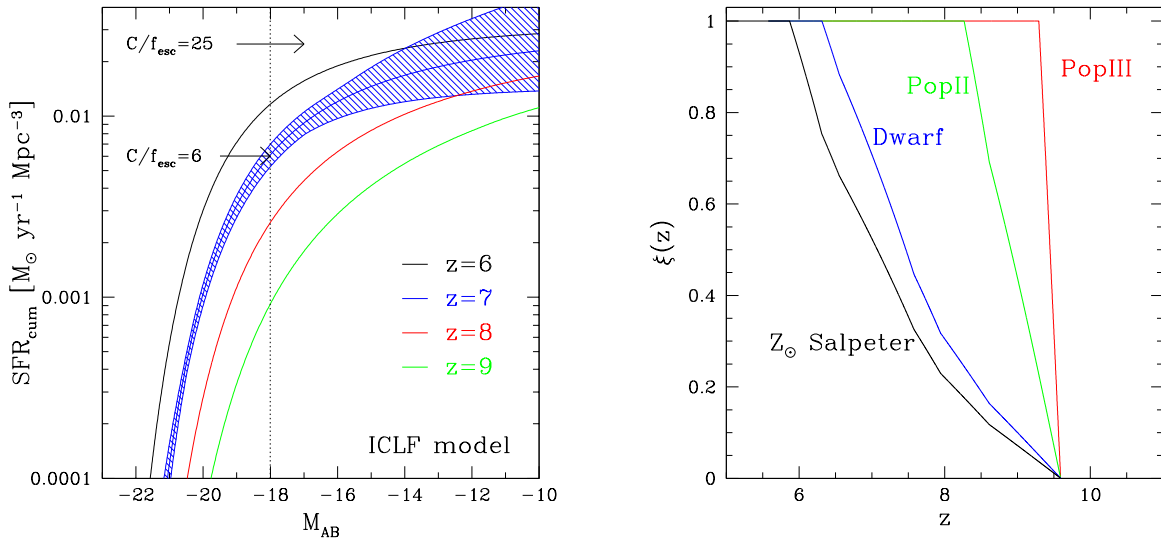


Fig. 3.— Left panel: Cumulative star formation rate for ICLF model with  $\Delta t = 200$  Myr. Blue-shaded area gives  $1\sigma$  uncertainty at  $z = 7$ . Critical reionizing SFRs for  $C/f_{esc} = 6$  and  $C/f_{esc} = 25$  at  $z = 7$  are indicated. Dotted line shows HUDF09 luminosity limit. Right panel: Evolution of IGM-mass reionization fraction  $\xi(z)$  for LFs shown in left panel, integrated to  $M_{AB} = -10$  under different SED assumptions (black:  $Z = Z_{\odot}$ , Salpeter; red: Pop III; blue: “dwarf”-like metal-poor [SED CS1 of Schaerer et al. 2003]; green: Pop II, top-heavy; see Stiavelli et al. 2004a).

Table 1. LF evolution

	CLF model			ICLF <sub>200Myr</sub> model			Observations		
	$(\phi_*)_{-3}^a$	$M_*$	$\alpha$	$(\phi_*)_{-3}^a$	$M_*$	$\alpha$	$(\phi_*)_{-3}^a$	$M_*$	$\alpha$
Input LF									
$z = 6$	1.4	-20.24	-1.74	1.4	-20.24	-1.74	$1.4 \pm 0.5$	$-20.24 \pm 0.19$	$-1.74 \pm 0.16$
Predicted LF									
$z = 4$	3.4	-20.81	-1.60	1.3	-20.90	-1.57	$1.3 \pm 0.2$	$-20.98 \pm 0.10$	$-1.73 \pm 0.05$
$z = 5$	2.3	-20.51	-1.66	1.5	-20.55	-1.63	$1.0 \pm 0.3$	$-20.64 \pm 0.13$	$-1.66 \pm 0.09$
$z = 7$	0.69	-20.00	-1.84	1.0	-20.00	-1.84			
$z = 8$	0.36	-19.75	-1.89	0.60	-19.70	-1.90			
$z = 9$	0.14	-19.50	-1.99	0.22	-19.55	-2.22 <sup>b</sup>			

Note. — Best-fit Schechter parameters for LFs in Figure 2 (second to fourth column: CLF model; fifth to seventh column: ICLF; last three columns: Bouwens et al. 2007 measurements). Fit holds for  $-22.5 \leq M_{AB} \leq -18$ . Relative residuals are  $\lesssim 20\%$ .

<sup>a</sup>Units:  $10^{-3} \text{ Mpc}^3$

<sup>b</sup>Asymptotic faint-end slope is  $\alpha \sim -2$

Table 2: Predicted dropouts for HUDF09 field

	Observed	ICLF <sub>200Myr</sub>	ICLF <sub>100Myr</sub>	ICLF <sub>300Myr</sub>	CLF
z-drop	16	$13.4 \pm 5.8$	$16.6 \pm 6.8$	$11.3 \pm 5.2$	$9.8 \pm 4.7$
Y-drop	5	$5.3 \pm 3.1$	$8.5 \pm 4.3$	$3.9 \pm 2.5$	$3.2 \pm 2.7$

Note. — Observed (Oesch et al. 2010b; Bouwens et al. 2010a) and predicted number counts for galaxies at  $z \sim 7$  (z-dropouts) and  $z \sim 8$  (Y-dropouts) in the HUDF09 field for different (I)CLF models. Predictions include convolution with effective HUDF09 volume as function of source magnitude.  $1\sigma$  uncertainty includes cosmic variance.